

# UTILITY OF MOTOR SPEED MEASUREMENTS IN PUMPING WELL ANALYSIS AND CONTROL \*

S. G. Gibbs

Nabla Corporation

## INTRODUCTION

The electrical prime mover on a rod pumped well is responsive to the load imposed on it. When load increases, the prime mover slows down. Similarly, when load decreases, the motor responds by speeding up. By virtue of the motor's reaction to load, motor speed can be used to diagnose operating conditions in the equipment and even to perform pump-off control and continuous monitoring.

This paper describes how motor speed can be used to deduce items of practical interest. With respect to equipment loading, gearbox torque can be deduced from motor speed and the relationship between speed and motor torque. Unit balance can be sensed and counterbalance can be adjusted to minimize loading and to conserve power. An unexpected result is that reasonably precise dynamometer cards can be inferred from motor speed and unit geometry, even without use of a dynamometer.

When suitable motor performance data are available (relationships between motor speed, torque, current and efficiency), a qualitative electrical analysis can be performed, even without electrical instrumentation. Power consumption, power factor, and current levels can all be inferred from motor speed and suitable manufacturer supplied data.

Using microcomputer technology, pump-off control can also be accomplished. Using speed and mathematical relationships between instantaneous output power and speed, the integrated motor output during a stroke is computed. Recognizing that motor output is used to 1) lift fluid and 2) overcome friction, the logic is applied that a decrease in motor output indicates a decrease in fluid lifted since friction is sensibly constant whether the well is pumped-off or not. The well is sensed to be pumped-off when motor output power (derived from speed) drops sufficiently below output power required when the well is on the verge of pumping-off.

In the context of continuous monitoring, motor speed can be used to infer rod parts, worn pumps, tubing leaks and responding wells.

\* SPE 13198—Presented at 59th Annual Technical Conference and Exhibition, Houston, TX., Sept. 16-19, 1984

The paper contains several comparisons of actual and inferred performance to demonstrate the utility and validity of the concepts.

## ELECTRICAL AND MECHANICAL PERFORMANCE OF INDUCTION MOTORS

Most beam pumping units are powered by three phase induction motors. Their electrical and mechanical behavior can be represented graphically as in Figure 1 which shows example curves for a 100 hp Nema D motor. In principle, all performance parameters can be inferred from three speed relationships with torque, line current and efficiency (Reference 1).

A key item is motor output torque. As shown in Figure 1, a large torque is produced at zero speed (locked rotor condition) which provides starting torque required for the pumping unit. Output torque is zero at synchronous speed. Should the motor be driven past synchronous by the counterweights, a negative braking torque is produced. In the operating range near synchronous, speed is seen to decrease as higher output torque demands are placed on the motor.

Line current is another important parameter shown versus motor speed in Figure 1. At locked rotor conditions, a large current is drawn. As motor speed increases, current decreases to a minimum value at synchronous (called the magnetizing current). Should the motor be driven by the pumping unit into the braking region, line current again begins to increase.

The ratio of output to input (efficiency) is the final parameter to be discussed. At locked rotor conditions, efficiency is zero because output is zero (the rotor is not turning). At synchronous speed, efficiency is again zero because output torque is zero. Efficiency rises to a maximum value between locked rotor and synchronous speeds. As Figure 1 shows, the efficiency can be very low at speeds near synchronous. This is why oversized motors which run too near synchronous speed tend to be less efficient than smaller motors which tend to run in a more optimum range of their efficiency curves. Should the motor be driven past synchronous speed, efficiency again rises to a local maximum and then declines at higher speeds.

The data of Figure 1 pertain to a specific motor. Other types and sizes of motors can have decidedly different performance curves. Furthermore, some of the data such as shown in Figure 1 must be assumed. For example, most motor manufacturers do not publish data in the regenerative braking region, so educated guesses on the part of the user are required. Also, performance data at low speed and at speeds very close to synchronous are usually not available.

Mechanical and electrical performance can be derived from performance data using simple equations and measured or predicted histories of motor speed. Average power at the output shaft during a stroke of the pumping is given by \*

$$P_o = \frac{1}{6600 \theta} \int_0^{2n\pi} T \, d\theta \quad (1)$$

This integral can be approximated by the sum

$$P_o = \frac{1}{63000 \, n} \sum_{j=1}^n T_j \, N_j \quad (2)$$

Since motor efficiency is also known as a function of speed, input power is approximated by the sum

$$P_i = \frac{1}{63000 \, n} \sum_{j=1}^n \frac{T_j \, N_j}{E_j} \quad (3)$$

When a motor is driven past synchronous speed, it generates power and returns it to the distribution system. Power companies usually install detented (ratcheted) meters which prevent credit being given for back driven power. Power consumption as indicated by detented meters can be computed with equation (3) by omitting from the sum any term involving a motor speed in excess of synchronous.

Motor loading is often inferred by comparing rated current with calculated root-mean-square current. RMS current can be derived from motor performance curves using the formula

$$I_{RMS} = \sqrt{\frac{1}{n} \sum_{j=1}^n I_j^2} \quad (4)$$

Power factor is another important parameter which can be inferred from performance curves. Power factor is the quotient of real and apparent power. Its instantaneous value is

$$F_{p_j} = \frac{746 \, T_j \, N_j}{63000 \sqrt{3} \, V \, I_j \, E_j} \quad (5)$$

Average power factor over a complete stroke of the pumping unit is usually taken as

$$\bar{F}_p = \frac{0.746 P_i}{\sqrt{(0.746P_i)^2 + (\text{KVAR})^2}} ; \text{KVAR} = \frac{3}{1000} \frac{V}{n} \sum_{j=1}^n I_j E_j \sqrt{1 - F_{p_j}^2} \quad (6)$$

where real input power  $P_i$  is given by equation (3) and instantaneous power factor  $F_{p_j}$  is given by equation (5).

## SOME PRACTICAL APPLICATIONS

### Electrical Predictions

Modern design methods for rod pumping equipment predict motor speed during a stroke of the pumping unit. This is made possible by including motor torque-speed characteristics in the mathematical model forming the basis of the design method (References 2 and 3). If motor speeds can be predicted with reasonable accuracy, graphical relationships between torque, efficiency and current (all versus speed) can be used to make electrical predictions with the simple equations just described. The predictions thus made are useful in minimizing energy costs and in selection of equipment.

Figure 2 shows predicted and measured motor speeds for a 5075 ft well equipped with the 100 hp motor of Figure 1. Using the process just described, the electrical predictions shown in Table 1 are obtained. As can be noted, there is good agreement between measured and predicted electrical performance.

### Electrical Analysis without Electrical Meters

The previous section describes how electrical predictions can be derived from performance curves and motor speed predictions. An inverse approach can be taken where actual speed measurements are made and electrical quantities are then derived from performance curves. This results in the interesting and useful procedure whereby an electrical analysis can be made without use of electrical measuring equipment.

Motor speed can be measured in a variety of ways. A common analog method involves a generating tachometer. Digital means are also applicable. A microcomputer-based method involves attachment of a magnet to the motor shaft or sheave. Then a Hall-effect transducer is used to sense the passing of the magnet as the motor revolves. Using its sense of timing, the microcomputer determines

the time required for each revolution of the motor and speed is inferred to a high degree of accuracy.

Using the digital method of measuring motor speed just described, the actual measurements of Figure 2 are combined with the performance curves of Figure 1 to produce the electrical analysis of Table 1. The analysis thus made is in good agreement, practically speaking, with actual measurements.

Tables 2 and 3 illustrate the hand calculation process for performing an electrical analysis. For brevity, only 25 motor speeds per pumping unit stroke are considered in these examples. In an actual case, more samples should be taken to increase accuracy.

Electrical measurements on a pumping well are difficult and costly to make, particularly if the well is unstable. The analysis method can be used to infer electrical quantities economically and rapidly - even from stroke to stroke.

#### Sensing Dynamometer Cards Without Use of Dynamometers

Mechanical loading on the pumping unit and rods can also be derived from the behavior of the electrical prime mover. A pumping unit motor feels torque imposed on it from rod loads, counterbalance effects, drive train inertias and friction. Motor torque related to rod load is influenced by the geometry of the pumping unit and by changing magnitude of the rod loads.

Counterbalance effects also exert torque on the motor and result from beam weights or revolving counterweights or air pressures. Drive train inertia effects are of lesser importance unless ultra high slip prime movers are being used. Friction is normally small and usually is neglected.

Using the concepts in Reference 4, the torques imposed on a motor driving a crank balanced unit are given by

$$T = \frac{1}{n} \left[ F_C (W_{PR} - F_{UB}) - M \sin (\theta + \beta) - I_1 \frac{d^2\theta}{dt^2} + \frac{F_C I_2}{L^2} \frac{d^2x}{dt^2} \right] \quad (7)$$

The above equation can be used to infer a dynamometer card from motor performance by solving for polished rod load

$$W_{PR} = F_{UB} + \frac{1}{F_C} \left[ n T + M \sin (\theta + \beta) + I_1 \frac{d^2\theta}{dt^2} - \frac{F_C I_2}{L^2} \frac{d^2x}{dt^2} \right] \quad (8)$$

Motor speed measurements are taken beginning at a known point in the stroke, say at bottom. The fundamental equation is phrased in terms of crank angle and velocity but similar quantities at the motor are obtainable with the simple formulas

$$N = n \frac{d\theta}{dt} ; \phi = n\theta \quad (9)$$

as long as the belts do not slip. The polished rod position  $x$  and the torque factor schedule  $F_C$  are related to crank angle through unit geometry. Finally, the phase angle  $\beta$  is determined from geometry to synchronize counterbalance torque with gravity and the beginning point of motor speed measurements.

This procedure is applied to the example 5025 ft well and the dynamometer cards of Figures 3 and 4 are constructed. Figure 3-a is the dynamometer card inferred from motor speed and Figure 3-b is the actual card measured with a dynamometer. The pump is filling completely with liquid. Figures 4-a and 4-b show similar cards in the same well in a pumped-off condition. The inferred dynamometer cards are calculated each 7-1/2 degrees of crank rotation.

The inferred and actual dynamometer cards are remarkably similar, even to the magnitude of the maximum and minimum loads. The inferred cards are not plotted near the ends of the stroke. This is because of equation (8) which becomes indeterminate when the torque factor  $F_C$  vanishes at the end of the stroke. Inertia effects are negligibly small because speed variations are small for the lightly loaded Nema D motor in use. It is remarkable that dynamometer cards can be inferred from motor speed with good clarity, even without aid of a dynamometer. Precision can be improved by computing the inferred cards on a more closely spaced crank angle grid.

#### Inferring Gearbox Torque and Unit Counterbalance Requirements from Motor Speed

Determination of gearbox loading and counterbalance requirements are among the most important activities in pumping well analysis. An obvious and somewhat simpler application of motor speed measurements is in determining gearbox load and counterbalance requirements.

Gearbox torque can be inferred from motor speed measurements using the following equation

$$T_{GB} = n T + I_3 \frac{d^2\phi}{dt^2} \quad (10)$$

The measured speed of Figure 2 and the torque-speed relationship of Figure 1 are used to compute the gearbox torque history of Figure 5 (curve a). Motor speed measurements are begun at the bottom of the stroke and inertia effects are neglected.

Peak gearbox torque of 672228 in-lbs inferred from motor speed compares favorably with peak torque of 662500 in-lbs calculated in the usual way from unit geometry and a measured dynamometer card. Figure 6 compares inferred torque and conventionally calculated torque, both plotted versus polished rod position. The shape of the plots is quite similar, although the inferred torque is somewhat more variable (the plot looks jagged). This is probably due to belt "whip" in the neighborhood of synchronous speed where torque is low and even changes sign (from plus to minus and vice versa). This causes the driving and driven belts to be alternately slack and taut and this behavior affects the measured motor speed.

From geometry considerations, the number of motor revolutions for the up and down stroke is known. For the conventional unit being studied, the upstroke requires about as many revolutions as does the downstroke. Since gearbox torque is computed beginning on the upstroke, it is known that the unit is underbalanced (more counterbalance effect is needed). This is evident because peak torque on the upstroke is greater than peak torque on the downstroke. Proper counterbalance can be inferred using the formula

$$T_{IB} = T_{GB} + M_c \sin(\theta + \beta) \quad (11)$$

In this relation, it is recognized that motor angle is related to crank angle by equation (9) as long as the belts do not slip. Counterbalance phase angle  $\beta$  is chosen to orient counterbalance effect with the beginning of the upstroke.

Figure 5 (curve a) shows the basic torque pattern with present counterbalance effect of 961500 in-lbs and how addition of a properly phased sinusoidal counterbalance torque of 80000 in-lbs (curve b) will properly balance the unit (curve c). In ideal balance, peak torque on the upstroke (599000 in-lbs) is equal to peak torque on the downstroke. Thus the total counterbalance required to balance the unit is 1040500 in-lbs (961500 + 80000). By balancing the unit in this manner, gearbox torque load has been reduced from 105% of rating to a less dangerous 93.6% of rating. Also, a small saving in power consumption will result.

The ideal counterbalance inferred from motor speed measurements (1040500 in-lbs) compares favorably with the ideal counterbalance of 1053000 in-lbs which is calculated from conventional methods using a dynamometer card and geometric torque factors.

Ammeters are often used to sense unit balance. Electrical balance is said to exist when peak current on the upstroke is found equal to peak current on the downstroke. Similarly, a unit is said to be electrically underbalanced when peak upstroke current exceeds peak downstroke current (and vice versa for electrical overbalance).

The same definitions apply to mechanical balance wherein peak torque is substituted for peak current. In some cases, the ammeter will not give a true indication of mechanical balance.

As Figure 1 shows, line current attains a minimum value at synchronous speed and increases into both the motoring and braking regions. Thus an ammeter cannot distinguish between motoring and generating currents.

If both upstroke and downstroke peaks occur with the motor operating below synchronous speed (motoring), the ammeter will give a valid indication of mechanical balance. If, however, one of the peaks occurs in the braking region (speed greater than synchronous), the ammeter will give a false indication of balance. This is because current increases while torque decreases in the braking region.

The method of sensing unit balance from motor speed measurements always gives a proper indication of balance, whether the motor is braking or motoring.

#### Pump-off Control Using Motor Speed Measurements

The basic role of a pump-off controller is to sense when a well begins to pound fluid so it can be shut down to allow further entry of reservoir fluids into the wellbore. Shutting the well down serves at least two useful purposes:

- 1) Power is saved, and
- 2) the damaging effects of overpumping (fluid pound and wear) are avoided.

Pump-off control can be performed using motor speed measurements and torque-speed relationships such as shown in Figure 1. These items are used with equation 2 to computer motor output power. Motor output power is used to do useful work in lifting fluid to the surface and to overcome friction losses. Because friction losses are practically constant whether the well is pumped-off or not, a decrease in motor output power usually heralds a decrease in fluid lifted, i.e., the well is pumping off. A speed-based controller is calibrated by computing reference output power with the well on the verge of pumping off. Pump-off is sensed when motor output power drops sufficiently below the reference, at which time the unit is shut-down.

To illustrate the method of sensing pump-off, Figure 7 is presented which pertains to a 5000 well equipped with a 144 inch

unit, a 2 inch downhole pump and a 75 hp motor. Pumping speed is about 10.3 strokes per minute. Figure 7-a shows surface and pump dynamometer cards as the unit starts up after a five minute downtime. Pump liquid fillage is complete and no fluid pound exists. Figure 7-b shows corresponding cards after the well has pumped 11 minutes, and a slight fluid pound has developed. Pertinent data are shown below:

	<u>NO</u> <u>FLUID POUND</u>	<u>SLIGHT</u> <u>FLUID POUND</u>
Instantaneous Production (BPD)	592	513
Motor output power (hp)	33.1	31.0
Pseudo motor output power (units)	662	620
Polished rod power (hp)	29.8	27.9
Friction losses (hp)	10.0	9.9
Useful downhole pump power (hp)	23.1	21.1
Average current (amps)	56.0	54.6

As the tabular data shows, motor power decreases (from 33.1 hp to 31.0 hp) as the well pumps off and begins to produce less fluid. By setting the threshold at 31.0 hp, the controller can be made to shut the well down with the slight fluid pound shown. As the well pumps off, the motor speed pattern changes during the stroke and equation 2 indicates a decrease in motor output power. To allow a microcomputer to use integer arithmetic, a pseudo power is often used which is a multiple of true power.

Dynamometer card shape is unimportant to a speed based pump-off controller. Thus, it can sense a fluid pound even if little evidence of it exists on the surface dynamometer card. This behavior is especially exhibited by fiberglass rods because they tend to mask the fluid pound (see Figure 8). Figure 8-a shows the well with a completely filled pump (well not pumped-off). Figure 8-b shows the same well with a slight fluid pound. The motor output power clearly indicates the pumped-off condition, although little evidence of a fluid pound exists on the surface card. Deep, slow pumping wells which are equipped with steel rods also show little evidence of a fluid pound at the surface, similar to fiberglass.

As mentioned previously, motor output is a predictable quantity. Figure 9 shows a theoretically determined relationship between motor power and pump liquid fillage expressed as a percentage. The relationship is non-dimensionalized, hopefully to make it apply to a broad spectrum of wells. Normal downhole friction is assumed.

Figure 9 is used as follows:

1. With downhole fillage complete (but with the well on the verge of pumping off), determine motor power using equation 2 and measured motor speed.

2. Form the ratio between motor power with the well pounding fluid and with full pump motor power determined in step 1 above.
3. Figure 9 is then used to compute approximate liquid fillage.

To validate the theoretically derived relationship, the actual surface and pump dynamometer cards of Figure 10 are presented. The pump cards are derived using the methods of Reference 5. Figure 10-a shows complete (100%) liquid fillage and a measured pseudo power of 382. The sequence continues through Figure 10-e which shows 49% pump liquid fillage and a pseudo power of 282. The theoretical curve is found reasonably precise by comparing the actual data of Figure 10 at various fillages. The largest error noted is about 4%.

The theoretical curve is determined using predictions of motor speed (References 2 and 3), equation 2 and performance curves such as shown in Figure 1. The fillage graph has utility in calibrating motor speed based pump-off controls and in the diagnostic sense of determining pump liquid fillage during routine pumping operations.

An example application of the fillage graph is as follows. Suppose that motor output power with a full pump (on the verge of pump-off) is 382. The problem is to determine approximate pump fillage when motor output is 350. The ratio  $350/382 = 0.916$  is formed and Figure 9 is used to estimate an approximate pump fillage of 83%. This compares closely with the actual fillage of 79% shown in Figure 10-c. As long as frictional effects are normal, the fillage graph is applicable to many wells in its non-dimensional form. As downhole friction increases beyond normal, the slope of the line in Figure 9 decreases.

#### Continuous Monitoring with Motor Speed Measurements

Wells can be continuously monitored using motor power as inferred from measured motor speed and torque-speed relationships. An important activity for a monitoring device is to sense when a rod part occurs and to alert operating personnel of the malfunction. Even though a speed based monitoring device employs no load cell, it can still sense a rod part. When rods part, a large decrease in motor output power occurs because fluid is no longer being lifted. The motor needs only to generate enough power to overcome drive train and downhole friction losses. Figure 11 shows the example well (of Figure 7) with a rod part at about 3300 feet. As noted, the unit is badly out-of-balance (overbalanced). Because of the out-of-balance condition, the motor must supply a large power output on the downstroke while lifting the weights. But on the upstroke, the weights drive the motor beyond its synchronous speed and a large amount of back-driven power is recovered. Thus, over a complete pumping stroke, net output power is very low.

With a rod part, the monitoring device finds motor power continuously low and a malfunction alert can be issued. The tabular information below summarizes the result.

With Rods Parted

Instantaneous Production (BPD)	0
Motor output power (hp)	11.9
Pseudo Motor output power (units)	238
Polished rod power (hp)	7.6
Friction losses (hp)	11.9
Useful downhole pump power (hp)	0
Average current (amps)	61.4

The above example shows why motor current pump-off controllers which relate pump-off to decreases in average current are unreliable. Even with parted rods, average current (61.4 amps) is higher than with a completely filling pump (56 amps). This is because ammeters are unable to distinguish between motoring and generating currents (see Figure 1).

In continuous monitoring, a key item is the amount of time that the well is pumped each day (and trends thereof). The extremes range from Minimum Pumping Time to Full Time Pumping. These are defined as follows:

- Minimum Pumping Time-- This occurs when the monitoring device elects to shut the pumping unit off soon after start-up.
- Full Time Pumping-- This occurs when the monitoring device elects to produce the well without a shutdown over a long period of time, say 24 hours or more.

Each of the above extremes can have diagnostic implications as follows:

Minimum Pumping Time--

- \*The rods may have parted. With parted rods, no fluid is being lifted and motor power is low causing the monitoring device to shut-off immediately after start-up.
- \*The fluid level may be high. Motor output power is low because the high fluid level is helping lift the well (not because the well is pumping off). This could be caused by a tubing leak, a check-valve leak, a completely worn-out pump, a recent power interruption, circulating the well or pronounced water flood response.

### Full Time Pumping--

\*Paraffin deposition may have increased downhole friction such that motor output power no longer drops below the cutoff level causing full time pumping.

\*The reservoir may be in the early stage of flood response. Pumping time has increased but fluid level is not yet high enough to cause Minimum Pumping Time.

\*A slight tubing leak may have developed such that the well needs to operate full-time. The rise in fluid level is not yet sufficient to cause Minimum Pumping Time.

\*The pump may be beginning to wear. Losses due to fluid turbulence in the pump are offsetting some of the power normally required to lift fluid. Pump condition has not yet deteriorated to the point that a high fluid level is causing Minimum Pumping Time.

A speed based monitoring device can be made to signal minimum or full-time pumping so that corrective action can be taken by operating personnel.

### CONCLUSIONS

1. Motor speed during a pumping unit stroke is indicative of operating conditions in the pumping equipment.
2. Speed measurements coupled with suitable motor performance data are useful in determining electrical power consumption, qualitative dynamometer cards, torsional analyses and counterbalance requirements. Continuous monitoring and pump-off control are also applications of the concepts described in this paper.
3. The techniques described herein are limited by the quality and availability of motor data. Motor manufacturers could make their information more pertinent if they would
  - a) publish performance data throughout the operating range starting at locked rotor conditions and continuing into the braking region;
  - b) use a uniform testing procedure so that different brands of motors could be meaningfully compared;
  - c) insofar as possible, indicate the likely effects on performance caused by temperature and voltage variations.

## NOMENCLATURE

L	=	pumping unit dimension from saddle bearing to horsehead arc, ft
E <sub>j</sub>	=	instantaneous efficiency of motor, %/100
F <sub>c</sub>	=	pumping unit torque factor, in
I <sub>j</sub>	=	instantaneous line current, amps
I <sub>RMS</sub>	=	root-mean-square motor current, amps
I <sub>1</sub>	=	moment of inertia of all rotary drive train elements (from counterweights to motor rotor) referred to slow speed shaft of speed reducer, slug-ft <sup>2</sup>
I <sub>2</sub>	=	moment of inertia of articulating elements referred to saddle bearing, slug-ft <sup>2</sup>
I <sub>3</sub>	=	Moment of inertia of drive train elements from motor rotor to slow speed shaft of gearbox (referred to motor rotor), slug-ft <sup>2</sup>
M	=	maximum counterbalance moment, in-lb <sub>f</sub>
M <sub>c</sub>	=	incremental amount of counterbalance moment required to balance unit, in-lb <sub>f</sub>
n	=	number of motor revolutions per stroke of the pumping unit
N or N <sub>j</sub>	=	instantaneous motor speed, rev/min
F <sub>p</sub>	=	average power factor during stroke of unit
F <sub>pj</sub>	=	instantaneous power factor
P <sub>i</sub>	=	input power to motor, hp
P <sub>o</sub>	=	output power of motor, hp
W <sub>PR</sub>	=	polished rod load, lb <sub>f</sub>
F <sub>UB</sub>	=	structure unbalance, lb <sub>f</sub>
t	=	time, seconds
T or T <sub>j</sub>	=	instantaneous motor output torque, in-lb <sub>f</sub>
T <sub>GB</sub>	=	gearbox torque (not necessarily in balanced condition), in-lb <sub>f</sub>
T <sub>IB</sub>	=	gearbox torque in balanced condition, in-lb <sub>f</sub>
x	=	position of the polished rod, ft
V	=	supply voltage, volts
B	=	counterbalance phase angle with respect to bottom of stroke, radians
θ	=	angular position of pumping unit cranks, radians
θ	=	period of pumping unit stroke, seconds
φ	=	angular position of motor rotor, radians

## REFERENCES

1. Howell, J. K. and Hogwood, E. E. Jr.: "Electrified Oil Production," The Petroleum Publishing Co., Tulsa, Oklahoma (1962).
2. Gibbs, S. G.: "Predicting the Behavior of Sucker Rod Pumping Systems," J. Pet. Tech. (July 1963) 769-78; Trans., AIME 228.
3. Gibbs, S. G.: "A General Method for Predicting Rod Pumping System Performance," paper SPE 6850 presented at the 1977 SPE Annual Technical Conference and Exhibition, Denver, Oct. 9-12.
4. Gibbs, S. G.: "Computing Gearbox Torque and Motor Loading for Beam Pumping Units with Consideration of Inertia Effects," J. Pet. Tech. (September 1975) 1153-59; Trans., AIME, 259.
5. Gibbs, S. G. and Nolen, K. G.: "Wellsite Diagnosis of Pumping Problems Using Mini-computers," J. Pet. Tech. (November 1973) 1319-23.
6. Neely, A. B. and Tolbert, H. O.: "Experience with Pump-off Control in the Permian Basin," paper SPE 14345 presented at the 1985 SPE Annual Technical Conference and Exhibition, Las Vegas, September 22-25.

Table 1  
Comparison of Measured Electrical Performance with Same Quantities  
Derived from Predicted and Measured Motor Speed

QUANTITY	ACTUAL	PREDICTED	INFERRED FROM MOTOR SPEED	REMARKS
INPUT POWER (TRUE KW)	20.78	20.7	23.3	EQUATION 1
INPUT POWER (DETENT KW)	NOT MEASURED	22.1	24.3	EQUATION 1 (PARTIAL SUMS OMITTED WHEN SPEED EXCEEDS SYNCHRONOUS)
OUTPUT POWER (HP)	NOT MEASURED	23.6	25.2	EQUATION 2
THERMAL CURRENT (AMPS)	55.58	57	53	EQUATION 4
PEAK UPSTROKE CURRENT (AMPS)	123	128	105	CURRENT CORRESPONDING TO MINIMUM UP-STROKE MOTOR SPEED
PEAK DOWNSTROKE CURRENT (AMPS)	90	93	84	CURRENT CORRESPONDING TO MINIMUM DOWN-STROKE MOTOR SPEED
MINIMUM POWER FACTOR (%)	0	0	0	EQUATION 5 (MINIMUM VALUE)
MAXIMUM POWER FACTOR (%)	88	86	86	EQUATION 5 (MAXIMUM VALUE)
AVERAGE POWER FACTOR (%)	NOT MEASURED	46	55	EQUATION 6
MONTHLY POWER BILL (\$)	913	909	1022	POWER COST BASIS: 6¢/KWH

Table 2  
Computation of Current and Power Factor

MEAS'MENT j (1)	SPEED rpm (2)	TORQUE in-lbs (3)	EFFIC. %/100 (4)	CURRENT amp (5)	CURR. x CURR. amp amp (6)	PWR FCTR %/100 (7)	NOTE 1 amp (8)
1	1203	-135	0.57	24.5	600	-0.17	13.8
2	1199	50	0.37	24.0	576	0.10	8.8
3	1189	460	0.79	26.2	686	0.39	19.1
4	1169	1285	0.85	35.5	1260	0.74	20.1
5	1149	2100	0.84	47.5	2256	0.90	17.2
6	1181	785	0.83	29.0	841	0.57	19.7
7	1200	0	0.00	24.0	576	0.00	0.0
8	1196	175	0.63	24.8	615	0.20	15.2
9	1197	130	0.57	24.5	600	0.17	13.8
10	1200	0	0.00	24.0	576	0.00	0.0
11	1198	90	0.53	24.2	586	0.12	12.8
12	1190	415	0.78	26.0	676	0.36	19.0
13	1187	540	0.80	27.0	729	0.44	19.4
14	1185	625	0.81	28.0	784	0.49	19.8
15	1185	625	0.81	28.0	784	0.49	19.8
16	1185	625	0.81	28.0	784	0.49	19.8
17	1173	1125	0.85	33.5	1122	0.69	20.5
18	1164	1495	0.84	38.5	1482	0.80	19.2
19	1186	590	0.80	27.5	756	0.47	19.4
20	1192	340	0.75	25.5	650	0.32	18.0
21	1184	665	0.81	28.2	795	0.51	19.6
22	1194	260	0.69	25.0	625	0.27	16.6
23	1211	-465	0.79	26.4	697	-0.40	19.1
24	1206	-270	0.69	25.0	625	-0.28	16.6
25	1203	-135	0.57	24.5	600	-0.17	13.8

SUM OF COLUMN 6: 20284

SUM OF COLUMN 8: 401.0

ROOT-MEAN-SQUARE CURRENT (see eq. 4)

$$I_{RMS} = \sqrt{\frac{20284}{25}} = 28.5 \text{ amps}$$

(A motor rated at 73 amps would be 39% loaded)

AVERAGE POWER FACTOR (see eq. 6)

$$KVAR = \frac{1.732(+60)(401)}{1000(25)} = 12.8 \text{ kilovolt amps reactive}$$

$$F_p = \frac{0.746(10.4)}{\sqrt{[.746(10.4)]^2 + [12.8]^2}} = 0.52$$

Note 1: Column 8 =  $I_j E_j \sqrt{1 - (\text{Column 7})^2}$ , see eq. 6  
Column 8 = (Column 5)(Column 4)  $\sqrt{1 - (\text{Column 7})^2}$

Measurements 1-12 are on upstroke.

This unit is mechanically and electrically underbalanced.  
KVA = 7.7(12.8) = 14.8 kilovolt amps

Table 3  
Computation of Input and Output Powers

MEASUREMENT j (1)	SPEED rpm (2)	TORQUE in-lbs (3)	SPEED x TORQUE rpm in-lbs (4)	EFFIC. %/100 (5)	SPEED x TORQUE / EFFIC. rpm in-lbs (6)
1	1203	-135	-162405	0.57	-284721
2	1199	50	59950	0.37	162908
3	1189	460	546940	0.79	691279
4	1169	1285	1502165	0.85	1774770
5	1149	2100	2412900	0.84	2882107
6	1181	785	927085	0.83	1119668
7	1200	0	0	0.00	0
8	1196	175	209300	0.63	334559
9	1197	130	155610	0.57	272809
10	1200	0	0	0.00	0
11	1198	90	107820	0.53	202061
12	1190	415	493850	0.78	631522
13	1187	540	640980	0.80	800825
14	1185	625	740625	0.81	914804
15	1185	625	740625	0.81	914804
16	1185	625	740625	0.81	914804
17	1173	1125	1319625	0.85	1559103
18	1164	1495	1740180	0.84	2078571
19	1186	590	699740	0.80	874238
20	1192	340	405280	0.75	543854
21	1184	665	787360	0.81	972530
22	1194	260	310440	0.69	449913
23	1211	-465	-563115	0.79	-711723
24	1206	-270	-325620	0.69	-471913
25	1203	-135	-162405	0.57	-284721

SUM OF COLUMN 4: 13327560

SUM OF COLUMN 6: 16342050

SUM OF COLUMN 6 WITH NEGATIVE QUANTITIES OMITTED FROM SUM: 18095130

OUTPUT POWER OF MOTOR (see eq. 2)

$$P_o = \frac{13327560}{63000(25)} = 8.5 \text{ hp.}$$

INPUT POWER TO MOTOR (see eq. 3)

$$P_i = \frac{16342050}{63000(25)} = 10.4 \text{ hp or } 7.7 \text{ kw}$$

INPUT POWER TO MOTOR MEASURED WITH RATCHETED METER

$$\frac{18095130}{63000(25)} = 11.5 \text{ hp or } 8.6 \text{ kw}$$

MONTHLY POWER BILL = 7.7 (24)(30.4)(0.06) = \$337 (\$376 with ratcheted meter) @ 6¢/kwh

$$\text{ELECTRICAL MOTOR EFFICIENCY} = \frac{100(8.5)}{10.4} = 82\%$$

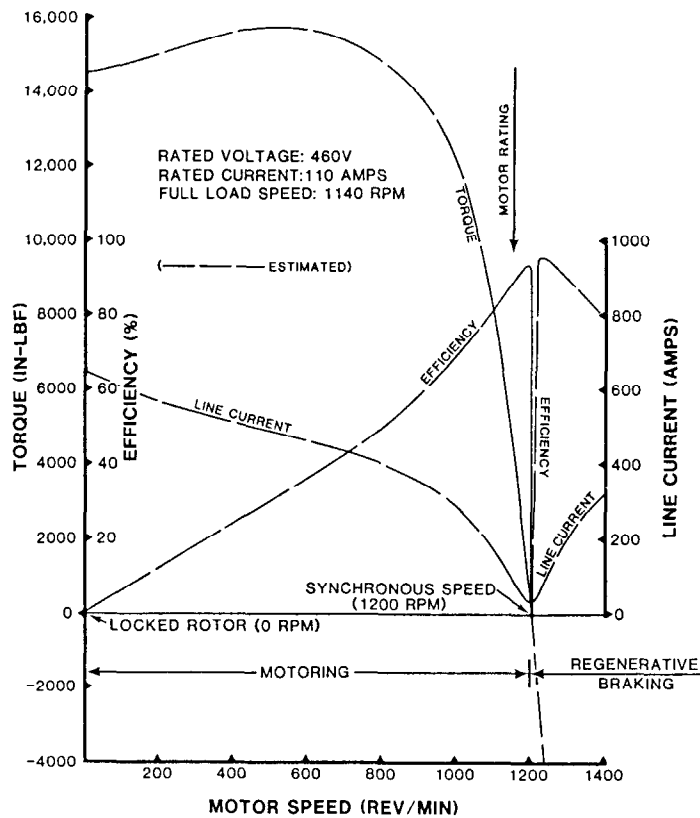


Figure 1—Performance curves for 100-hp Nema D motor

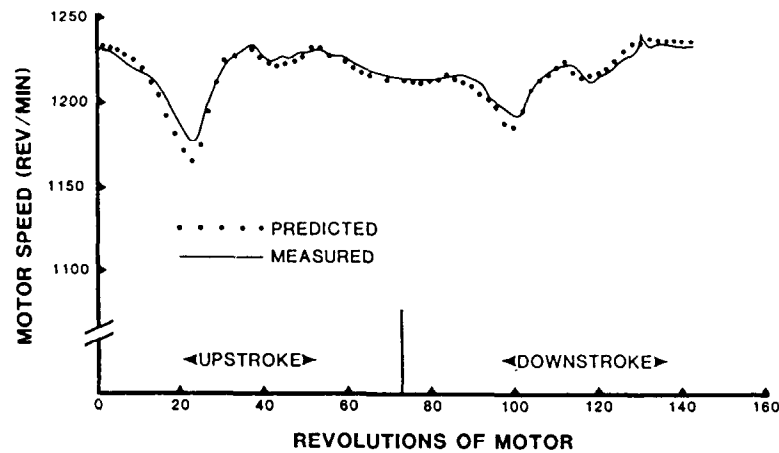


Figure 2—Measured and predicted motor speed in a 5,025-ft well

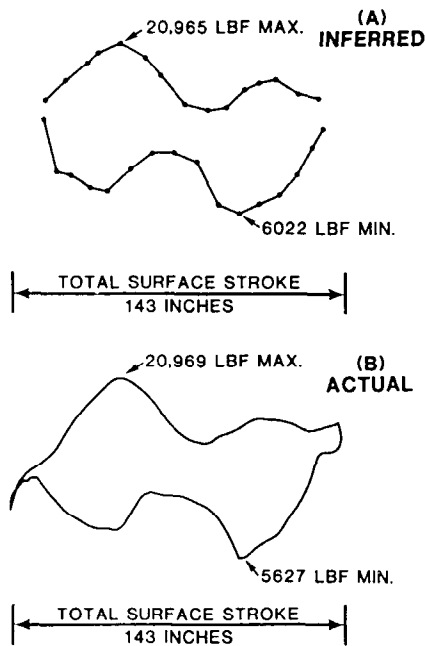


Figure 3—Comparison of actual dyno card with dyno card inferred from motor speed (full pump fillage)

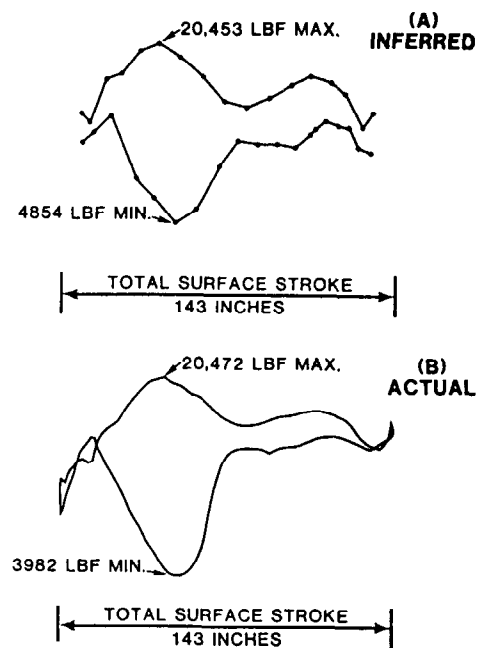


Figure 4—Comparison of actual dyno card with dyno card inferred from motor speed (severe fluid pound)

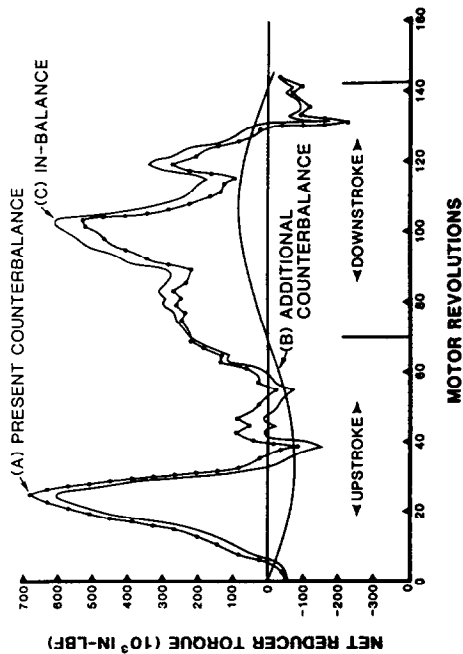


Figure 5—Gearbox torque and balancing requirements inferred from motor speed measurements

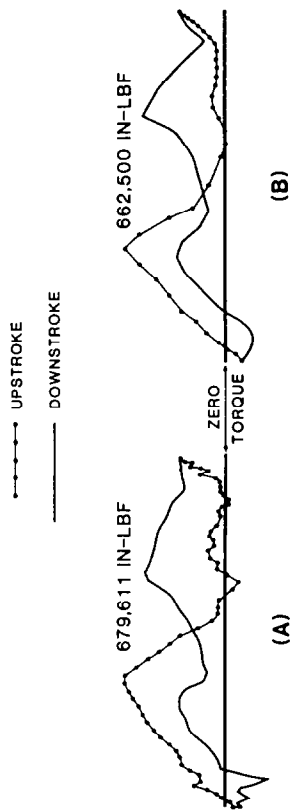


Figure 6—Comparison of torque/position plots inferred from motor speed and calculated in conventional manner

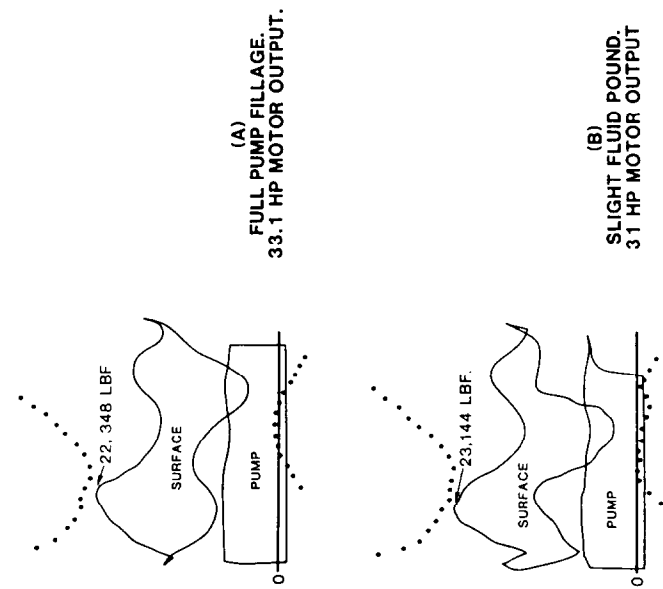


Figure 7—Dynamometer cards in a 5,000-ft well showing motor power decrease with pumpoff

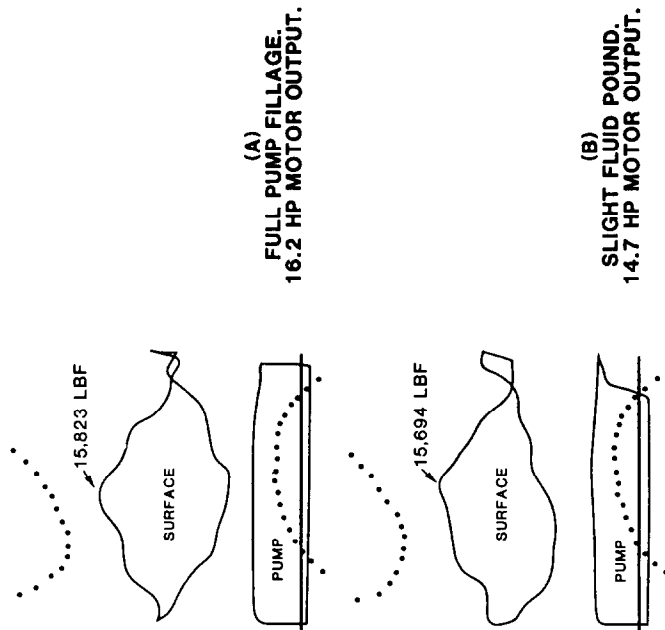


Figure 8—Dynamometer cards in 8,000-ft well equipped with fiberglass rods which mask fluid pound

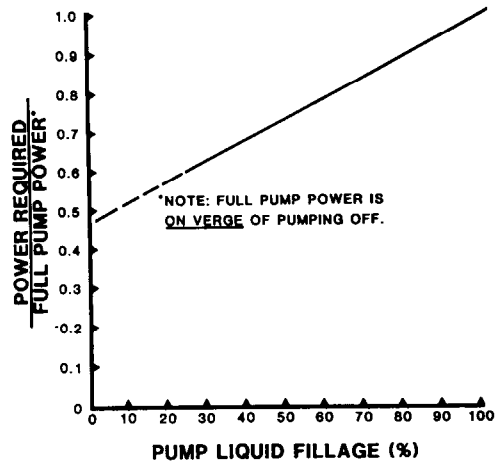


Figure 9—Approximate relationship between power ratio and pump liquid fillage

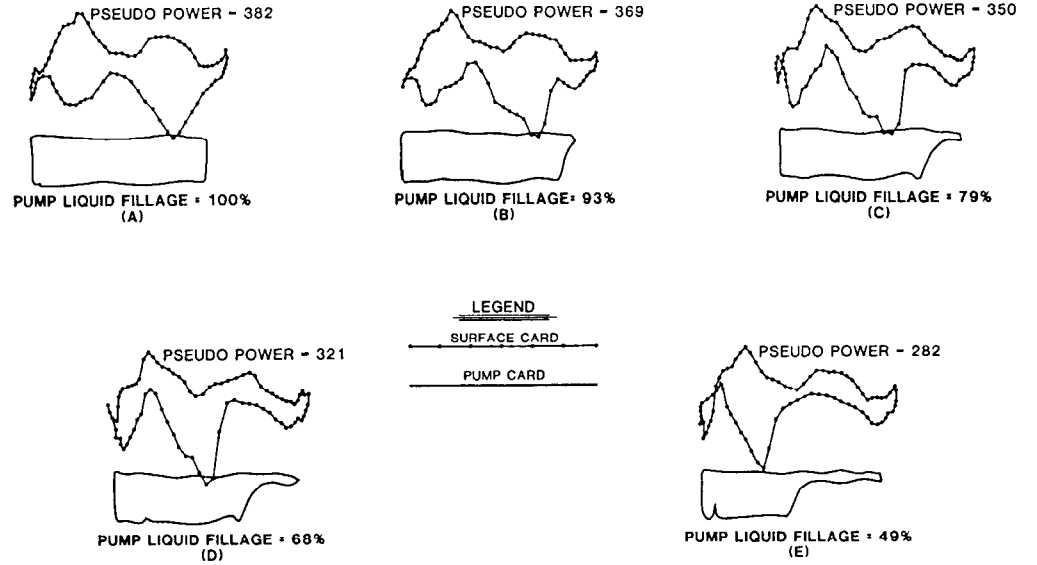


Figure 10—Actual dynamometer cards showing relationship between motor power and pump fillage

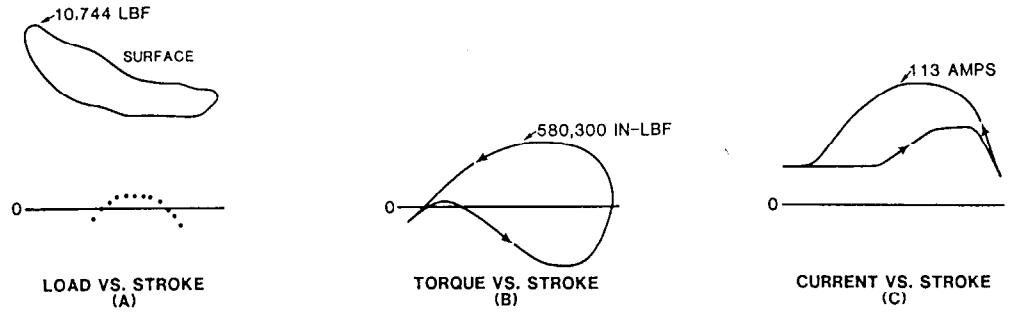


Figure 11—Dynamometer, torque, and current plots (parted rods at 3,300 ft)